22 November 1996

ELSEVIER

Chemical Physics Letters 262 (1996) 573–582

CHEMICAL PHYSICS LETTERS

Observation of coherent multiple scattering of surface plasmon polaritons on Ag and Au surfaces

Weining Wang, Mark J. Feldstein, Norbert F. Scherer [1]

Department of Chemistry, University of Pennsylvania, Philadelphia, PA 19104, USA

Received 19 January 1996; in final form 5 September 1996

Abstract

We report the observation of coherent multiple scattering of surface plasmon polaritons in Ag and Au films through attenuated total reflectance in the Kretschmann geometry. The pump–probe measurements reveal exponential tails in the amplitude of the reflected light that extend well beyond the pulse correlation time. The exponential tails reflect the temporal decay of surface plasmon polaritons (SPP). This observation and interpretation of SPP decay through scattering from surface roughness suggest the possibility of SPP localization on metal surfaces. An alternative interpretation of the signals, pulse reshaping due to the constant angle SPP modes, is ruled out.

1. Introduction

One of the most important issues in the study of surfaces and interfaces is how structural features, such as roughness, influence surface properties [1–4]. It has been recognized for a long time that many surface processes occur in association with irregular structural features (i.e., defects, steps, protrusions, etc.) rather than at atomically smooth planes [1–4]. This is one contributing factor to the increasing interest in the optical study of surface plasmon polaritons (SPP's). As surface electromagnetic waves, SPP's are very sensitive to the condition of a surface or an interface [1]. This sensitvity offers unique possibilities to observe material and topographical properties of surfaces and/or interfaces. In particular, Specht and coworkers resolved surface structures with 3 nm resolution by using a scanning tunneling microscope tip to modulate the SPP field [2]. Furthermore, it has been shown that surface roughness causes the formation of localized SPP's that may, in turn, strongly enhance certain surface processes, such as Raman scattering [3] and multiphoton photoemission [4]. These studies, performed with surfaces that were intentionally roughened either by electrochemical methods or by controlling the deposition conditions, had irregular features on the order of 10 nm or less. The enhancement of the surface optical and ionization responses was deduced from a comparison between roughened and unroughened surfaces.

Very recently, photon scanning tunneling microscopy was used to show that localized SPP's may be generated in room temperature deposited gold films [5]. In these films, only larger, e.g. 50–1000 nm in size and 5–100 nm in height, surface features exist. The experimental results suggest the existence

[1] National Science Foundation National Young Investigator.

PII S0009-2614(96)01113-X

of localized SPP's, which could be seen as local bright spots. Physically, the localized SPP's in both cases are the result of coherent multiple scattering of the delocalized SPP's by the random distribution of surface features.

Coherent multiple scattering and its relation to the localization of light in random media have been discussed extensively [6–10]. Most of these studies, both experimental and theoretical, were carried out with bulk materials. The photon scanning tunneling microscopy work [5] was a direct observation of light localization on surfaces. The recent work on 'diffusing-wave spectroscopy' by Yodh and coworkers [11] and imaging methods through random media including biological tissues by Alfano and coworkers [12] and Fujimoto and coworkers [13] is closely related.

The most widely used method in generating and monitoring SPP's are the attenuated total reflection (ATR) methods developed by Otto [14] and Kretschmann [15]. Surface roughness has been studied by measuring the directional scattered light [16,17]. Roughness has also been studied in connection with the propagation length or the temporal decay time of SPP's since the propagation length is sensitive to the surface features [1]. Earlier measurements of the SPP decay length have been performed in the Otto configuration at IR wavelengths because the decay length in this wavelength region is long [18]. Recent efforts in determining the decay length of SPP's in the visible have been successful; measurements at 632 nm and in the IR at 1064 nm have been reported using a scanning tunneling microscope and by an optical method utilizing CCD detectors [19]. All of these studies have been carried out with CW lasers to characterize the effect of surface roughness on the measured damping of the propagating SPP's that was measured.

When combined with femtosecond lasers, the ATR methods have the potential for directly providing information on dynamical processes occuring on surfaces. In the work of Groeneveld et al [20] time-resolved ATR in the Kretchmann configuration has been used to study the relaxation of hot electrons which were generated by the decay of SPP's in Ag and Au films [20]. We have also explored the SPP-assisted responses of thin Ag films with combined femtosecond pulse correlation techniques and both STM detection and STM-induced optical responses [21]. In this letter we report on a time-resolved study of coherent multiple scattering of SPP's in Ag and Au films and the measurement of the temporal decay times (i.e., momentum decay times) of these SPP's.

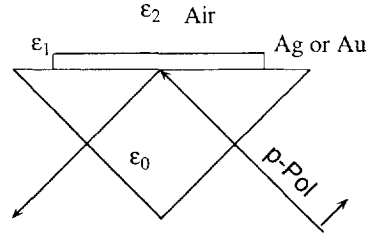

Fig. 1. Illustration of the ATR device. Prism with dielectic constant ϵ_0, metal film with dielectric constant ϵ_1, and air with ϵ_2. Arrows indicate direction of incident and reflected optical fields.

2. Experimental

The laser system used in this study was a home built Ti:Sapphire laser [21] pumped by an argon ion laser. The pulse duration for the experiments reported here was either 50 fs or 30 fs. The experimental setup for ATR studies is shown in Fig. 1. A more detailed description of the experimental setup has been reported elsewhere [21]. The samples were Ag films (50 nm and 35 nm thickness) and Au films (35 nm thickness) vacuum deposited directly onto the hypotenuse of fused silica or BK-7 prism substrates. The laser output was split into pump and probe beams by a 50% beamsplitter. The intensity of the probe beam was attenuated to about 10% of the intensity of the pump. The pump and probe beams were slightly displaced horizontally so that the pump could be blocked with an aperture after the sample. The p-polarized pump and probe beams were focused into the sample by a 5 cm focal length achromatic lens. The spot size at the sample was about 15 mm. After the sample a dark line could be seen in the reflected beams. This dark line corresponded to the resonant angle at which all the incident light was converted into SPP's, which propagate along the surface [1].

After the sample, and following 10 × beam expansion, the probe beam was collimated to about 1″ in diameter. An iris diaphram was used to select a

10^{-3} rad portion of the probe beam slightly off center of the 'dark band'; thus only light reflected in a well defined direction (and thus with a well defined k vector) was collected. The selected portion of the probe beam was detected by an amplified photodiode (Thorlabs). A long pass filter was used in front of the detector to block any second harmonic light generated at the surface. A glass slide was used before the sample to reflect a portion of the probe beam, which was sent to a second photodiode and used as a reference. The signal and reference photodiode outputs were sent to a digital lockin amplifier (Stanford Research 850), which was synchronized to the chopper modulation of the pump beam. The lockin was set to process either the signal for X or R, where $X = R\cos\phi$ and ϕ reflects the phase angle difference between the signal and the chopper reference and R is the magnitude.

3. Results

The pump–probe signal shown in Fig. 2a detected near the dark band is seen to contain interference fringes. The waveform was obtained by measuring the amplitude of the interference fringes as a function of the delay of the probe pulse [22]. The electric field interferometric nature of the signal is clear from the approximately equal positive and negative amplitude of the detected response. The interference results when pump light is scattered into the direction of the probe beam and interferes with the latter at the detector. If the aperture before the detector (i.e. photodiode) was adjusted to select a portion of the probe beam away from the dark band, only the pump-probe pulse correlation response was observed (Fig. 2b). This occurs because the portion of the probe beam away from the dark band consists almost entirely of specularly reflected light. By contrast, the response after about 50 fs in Fig. 2a, ontained detecting slightly off the center of the dark band, originates from the excitation of SPP modes.

Fig. 3a shows the temporal response obtained for the 50 nm thick Ag film with the lockin set for dectection of the magnitude of the interference fringes (i.e., detect R). The signal contained an instantaneous peak at $t = 0$ and an exponentially decaying tail. Fig. 3b and 3c present the data for a 35 nm thick

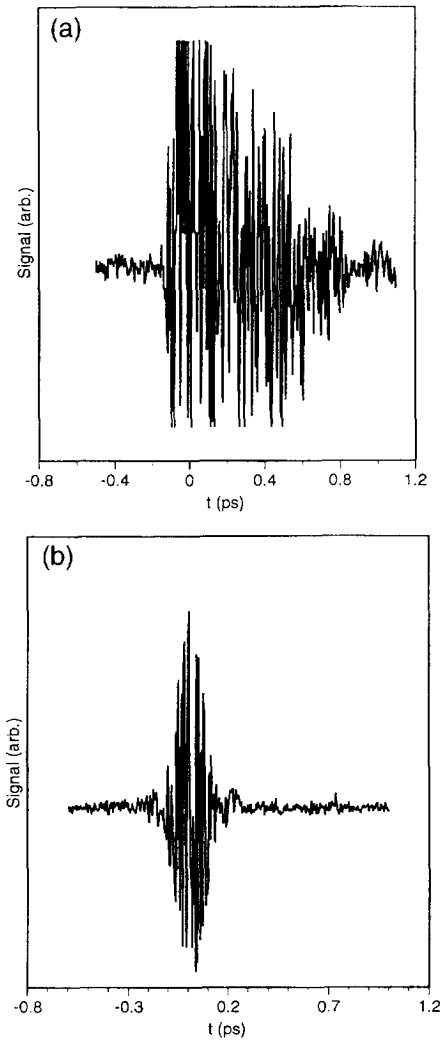

Fig. 2. a) A representative interferometric response measured with lockin amplifier set to detect X. The photodiode/aperture were positioned to detect at a point 10^{-3} rad form the dark band. b) Same as a) except detecting a portion of probe beam away from ATR resonance (i.e. the dark band).

Ag film and a 35 nm thick Au film, repectively. Fig. 3 also shows the simulated data using a photon diffusion model. As discussed below this exponentially decaying part results from the coherent multiple scattering of the SPP's generated by the pump pulse. The exponential decay corresponds to the inelastic (absorption and radiative decay) decay time of the SPP's on the surface. Each data set is an average of 10 individual scans.

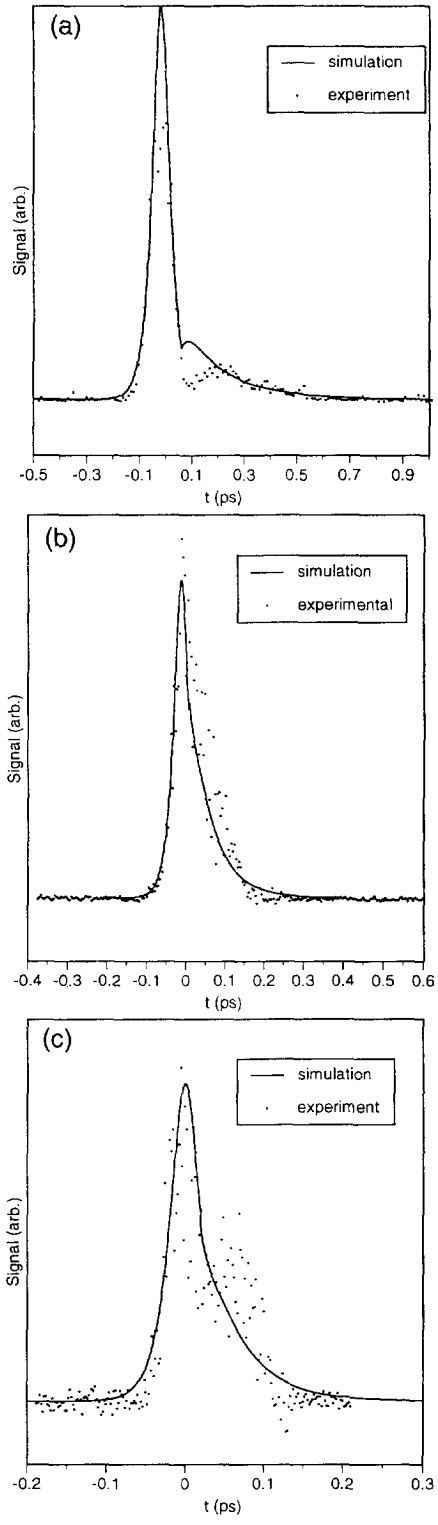

4. Discussion and model calculations

The signals shown in Fig. 2 and 3 are purely interferometric. The interference nature of the experimental signal was further demonstrated by using a piezotransducer in the pump arm. When the piezo was modulated with an amplitude adjusted to give a rapid 2p phase scan, thereby averaging over the phase difference between the pump and probe pulses at each delay, the interference fringes disappeared and the signal averaged to a flat base line. This pure interferometric signal away from the zero of time indicates that the measured response does not result from 'typical' population excitations, such as electron–hole pairs or electronic populations in impurity or adsorbed molecules. If the signal comes from any of the above mentioned excitations, then averaging over the phase difference between pump and probe would get rid of the interference fringes but show the population relaxation. Excitation of a traveling (transverse) wave material mode would behave differently than these point dipole excitations. The suggestion made by Groeneveld et al [20], who also observed an interference signal around $t = 0$, was that the interference resulted from surface roughness-induced scattering of the pump light into the probe direction. They did not resolve any temporal features presumably because of the longer pulse duration used in their experiment as well as shorter SPP momentum decay time at their wavelength. Here, with a 6-fold shorter pulse duration and a more favorable wavelength (i.e., 760 nm), this interference signal is temporally resolvable facilitating a better demonstration of the process involved.

The scattering of pump light into the probe causing in a signal around time zero is understood as

Fig. 3. Pump–probe response obtained by detecting near the dark band and lockin set to process the absolute magnitude of the signal, R, for various films. a) Experimental and calculation results for a Ag sample of 50 nm thick. Pulse duration 50 fs. b) Experimental and calculation results for a Ag sample of 35 nm thick. Pulse duration 30 fs. c) Experimental and calculation results for a Au sample of 35 nm thick. Pulse duration 30 fs. Solid line: calculation, points: experimental data. In all cases the calculated signal is the reshaped 'pump' pulse convoluted with the un-reshaped (and specularly reflected) probe pulse. Positive time then refers to the probe pulse field temporally overlapped with the delayed portion of the pump field.

resulting from the so called coherence coupling effect (i.e. sometimes termed coherence artifact) [23]. Observation of interference after time zero reveals more physical content. The interferometric nature of the response implies that optical phase coherence between pump and probe persists for more than several hundred femtoseconds. Optical dephasing times for chromophores in solution [24–27] as well as for some semiconductors [28] and metals [29] are known to be significantly less than 100fs. In degenerate electron systems, such as metals and some semiconductors, carrier–carrier scattering may be inhibited near the Fermi edge to allow long thermalization [30] and dephasing times [31]. However, since this latter process is not surface specific and requires cryogenic conditions and since in the present case no long time response was observed when the laser beam was detuned from ATR resonance (supra vida), this possiblility can be ruled out.

The long time delayed interference response can be caused by elastic scattering of light only in the strong multiple scattering regime where photon transport becomes diffusive [9]. If this is the case then the aforementioned results indicate that the SPP's generated are at least weakly localized. However, there is a second possibility which could also lead to a pure interferometric signal. This is the temporal pulse reshaping effect [32] of a smooth surface. This type of pulse reshaping effect is caused by the excitation of the so called 'constant angle' surface polariton mode [33]. Under certain circumstances [32], the effect may give a signal very similar in shape to the ones observed here. In this case, the spike around $t = 0$ would result from the specularly reflected part of the pump pulse, the trailing exponential tail would come from reradiated light by the constant angle SPP mode, which has been excited by the pump pulse, and the decay in the signal would reflect the lifetime of this mode.

The appearance of a second peak in the data of Fig. 3a,b, which is not observed in the interferometric data of Fig. 2a, can be attributed to a phase difference between the $t = 0$ coherent coupling peak (i.e. pump beam coupled into the probe direction) and the exponentially decaying signal. The interferometric data fluctuates too rapidly (i.e. it is sensitive to the changing relative optical phase between pump and probe pulses) to allow detection of this phase shift. The amplitude-averaged data, however, exhibit the dip in signal and distructive interference between the prompt scatter and the delayed yet coherent scatter (see discussion below).

4.1. Temporal pulse reshaping

Since it is difficult to discriminate between the two mechanisms on the basis of qualitative arguments, a demonstration that the signals are the result of coherent multiple scattering requires calculation of representative signals for each case and comparison with the experimental data. The temporal reshaping signals are calculated as follows.

The reflected light field can be described as

$$E_r(t) = \frac{1}{2\pi}\int_{-\infty}^{\infty} E_r(\omega)\exp(-i\omega t)\,d\omega, \tag{1}$$

where

$$E_r(\omega) = R(\theta,\omega)\,E_i(\omega), \tag{2}$$

with $E_i(\omega)$ the frequency domain representation of the input optical field and $R(\theta, \omega)$ the Fresnel factor for p-polarized light incident at an angle q in the Kretschmann geometry. The latter is given by [1]

$$R(\theta,\omega) = \frac{r_{01} + r_{12}e^{2ik_{z1}d}}{1 + r_{01}r_{12}e^{2ik_{z1}d}} \tag{3}$$

and

$$r_{ij} = \frac{\dfrac{k_{zi}}{\epsilon_i} - \dfrac{k_{zj}}{\epsilon_j}}{\dfrac{k_{zi}}{\epsilon_i} + \dfrac{k_{zj}}{\epsilon_j}} \qquad i,j = 0,1,2 \tag{4}$$

where the wavevector

$$k_{zi} = \left(\frac{\omega}{c}\right)\left[\epsilon_i - \epsilon_0\sin^2\theta\right]^{1/2} \qquad i = 0,1,2 \tag{5}$$

and d is the thickness of the metal film. The dielectric constant of the ith material phase is ϵ_i (i = 0,1,2). The dielectric constant of quartz (i.e. for the prism) is $\epsilon_0 = 2.296$, while $\epsilon_2 = 1$ for air. For the metal phase, $\epsilon_1(\omega) = \epsilon_1'(\omega) + \epsilon_1''(\omega)$. The Drude model is used to evaluate ϵ_1, that is

$$\epsilon_1(\omega) = 1 - \frac{\omega_p^2}{\gamma^2 + \omega^2} + i\frac{\gamma\omega_p^2}{\omega(\gamma^2 + \omega^2)}, \tag{6}$$

with ω_p (the plasmon frequency) and γ (damping constant) being 8.987 and 0.021 eV, respectively, for Ag and 9.028 and 0.080 eV, respectively, for Au. The dielectric constants for Ag and Au calculated from these values are well within the range of experimental values for Ag and Au given by Christy and Johnson [34]. With these relations and the material parameters, the reflected pulse shape can then be calculated by Eq. (1).

The frequency dependence of Eq. (2) on the incident radiation is analyzed by expanding it around ω_0. To first order, the resulting equation becomes

$$R = 1 - \frac{2i\gamma^{rad}}{\omega - \omega_0 - \omega^{rad} + i(\gamma^{int} + \gamma^{rad})}, \tag{7}$$

where

$$\gamma^{int} = -\frac{\epsilon_1''(\omega_0)}{\left.\frac{d\epsilon_1'}{d\omega}\right|_{\omega=\omega_0}} \tag{8}$$

and

$$\gamma^{rad} = \mathrm{Im}\left\{-\frac{4\epsilon_i'^2 r_{01} e^{2ik_{z1}d}}{(1-\epsilon_1')\left.\frac{d\epsilon_1'}{d\omega}\right|_{\omega=\omega_0}}\right\} \tag{9}$$

are the intrinsic and radiative damping constants, respectively. Finally,

$$\omega^{rad} = \mathrm{Re}\left\{-\frac{4\epsilon_i'^2 r_{01} e^{2ik_{z1}d}}{(1-\epsilon_1')\left.\frac{d\epsilon_1'}{d\omega}\right|_{\omega=\omega_0}}\right\} \tag{10}$$

is the shift of the resonant frequency (i.e., $\omega_0 + \omega^{rad}$ is the resulting resonant frequency) The lifetime of the constant angle SPP mode can be calculated from Eqs. (8) and (9) directly.

Table 1 lists the lifetimes of the constant angle mode SPP's for the three samples. Fig. 4 shows the calculated signals for values of θ at the associated ATR resonance angles, which correspond to the actual experimental conditions. The calculated pulse shapes are seen to be quite different from the experimental data. This is mainly a consequence of the very short lifetimes for the constant angle SPP modes in these films. We have also calculated the signal for a fictitious film with adjustable dielectric constant and thickness. Obtaining calculated lifetimes that are comparable to the measured data requires both reducing the damping constant in Eq. (6) and hence the imaginary part of the metal dielectric constant and increasing the thickness of the film to values far away from being realistic. For example, an 'Ag' film with a thickness of 80 nm and a γ of about 0.004 would give (from Eqs. (8) and (9)) a radiative lifetime of 510 fs and an intrinsic lifetime of 329 fs, yielding a lifetime of about 200 fs. With this choice of parameters the pulse reshaping mechanism would reproduce the 50 nm thick Ag signal very well. However, these chosen parameters are well beyond the experimental error in the knowledge of the film thickness and the actual damping constant of Ag and therefore do not correspond to the real experimental conditions. The analysis given here, therefore, provides quantitative evidence to eliminate pulse reshaping as the mechanism for the observed signals.

Table 1
Calculated lifetimes of constant angle SPP's

	τ_{rad} (fs)	τ_{int} (fs)	τ_{total} (fs) [a]
Ag 50 nm	34	62	22
Ag 35 nm	8.6	62	7.5
Au 35 nm	9.4	9.4	4.7

τ_{int}: intrinsic lifetime for the constant angle mode.
τ_{rad}: radiative lifetime for the constant angle mode.
$\tau_{total}^{-1} = \tau_{rad}^{-1} + \tau_{int}^{-1}$.
[a] Note comparison with fitted decay times listed in Table 2.

Before proceeding to the second possible mechanism for the source of the delayed but coherent light from the SPP it is useful to consider the effect of surface roughness on pulse reshaping. Mesoscopic roughness introduces an interesting complication that would be interesting to investigate numerically. On a rough surface the combination of spatial dispersion and the surface structural features may result in the creation of new modes that do not exist in the local mode model described above. Nevertheless, an argument can be made why the roughness will not solve the dilema of only being able to fit the data with unphysical parameters. First, non-locality is expected to be important in the large wave vector regime (or strongly dispersive regime in the case of the SPP), which is not the case here. Second, it is well known that surface roughness results in broadening of the

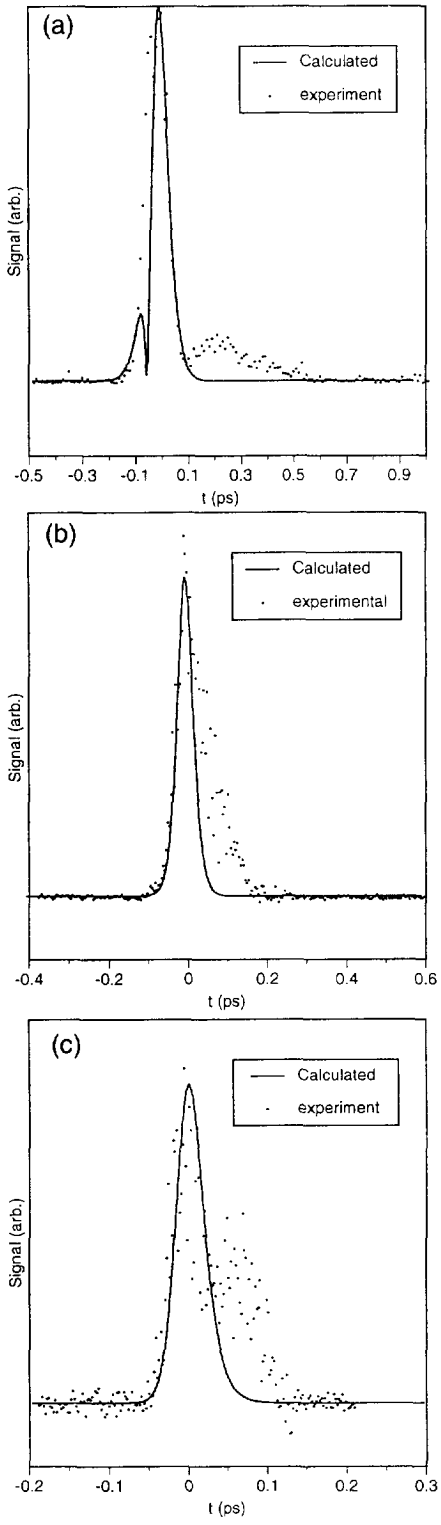

Fig. 4. Calculated signals for the pulse reshaping mechanism. (a) 50 nm Ag. Pulse duration 50 fs. (b) 35 nm Ag. Pulse duration 30 fs. (c) 35 nm Au. Pulse duration 30 fs. Experimental data (points) from Fig. 3 are superimposed for comparison.

ATR angular resonance [1,16,17] which results from the relaxed momentum and energy conservation constraints in the dispersion relation. In other words, surface polaritons are expected to be more strongly damped when there is spatial dispersion; the radiative damping parameter increases due to light emmission into the air side of the ATR device. Thus, consideration of the interaction of the electric field with mescopic (i.e. $< \lambda$ in size) non-uniformities will only case the pulse reshaping model to be even less applicable to explaining the current experimental data.

4.2. Coherent multiple scattering

A simple two dimensional diffusion model is used. Scattering of the propagating mode can be described as a two dimensional diffusion problem since an ATR device couples a light pulse into the surface and creates a surface plasmon polariton pulse which propagates along the surface. From a particle point of view, after having been coupled into the surface, the photons stay on the surface and are scattered around by the surface structures. If the scatterers are packed densely enough, some photons will be scattered back to the origin and establish an effective diffusive behavior. An illustration of this idea is given in Fig. 5. The diffusion equation for this motion is

$$\frac{\partial \Phi}{\partial t} = D\nabla^2\Phi - \gamma\Phi + N\delta(x)\delta(y)\delta(t), \qquad (11)$$

where Φ is the photon density, D is the diffusion constant, and $\gamma = 2/\tau$ is the damping constant which describes losses due to absorption and scattering out of the surface and τ is the amplitude temporal decay time. This equation has solutions of the form

$$\Phi = NG_x(x,t)G_y(y,t)e^{-\gamma t}, \qquad (12)$$

where N is a constant and G_x and G_y are the Green's functions for the one dimensional homogeneous diffusion equation. (This diffusion equation

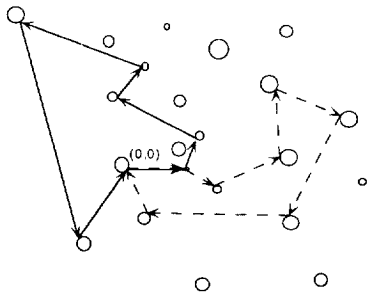

Fig. 5. Illustration of multiple scattering of light. Solid and dashed lines represent two different multiple scattering paths, both of which start from (0,0) and return to (0,0).

and its solution can be found in standard mathematical physics textbooks.)

In this case, since the photon pulse is generated directly within the random medium rather than through a boundary, an initial condition rather than a boundary condition exits. For simplicity, it is assumed that the initial condition is $\delta(x,0)\delta(y,0)$, which corresponds to a d pulse in time at location (x, y). Assuming further that the pulse is created at the origin, one obtains the solution

$$\Phi(x=0,y=0;t) \propto \frac{1}{4\pi Dt} e^{-\gamma t}. \tag{13}$$

The time-dependence of the scattered electric field is therefore

$$E(t) \propto \sqrt{\Phi(x=0,y=0;t)} \propto \sqrt{\frac{1}{4\pi Dt}}\, e^{-t/\tau}, \tag{14}$$

and the total reflected field is proportional to the superposition of the field given in Eq. (14) and the specularly reflected field E_0

$$E_{\text{total}}(t) \propto \alpha E_0(t) - \beta E(t), \tag{15}$$

where α and β are proportionality factors.

Since the experimental results were not calibrated to give the absolute magnitude of the electric field, it was not possible to extract the photon diffusion constant from Eq. (15). The fitted signals using Eq. (15) for the three samples are the solid lines in Fig. 3 shown there along with the experimental data points for comparison. The experimental data are well fit with the diffusion model. From the fitted curves, one can extract the temporal decay time τ. These values are listed in Table 2 along with the calculated propagation lengths on smooth metal surfaces and the temporal decay times of SPP's as determined by these propagation lengths [15]. On a rough surface the decay time is expected to be shorter [1] which is consistent with our experimental data. (Independent measurements of the STM topography of films obtained with the same deposition conditions show considerable roughness on nanometer and 10's of nanometer scales.)

Comparing the values for the decay times shown in Tables 1 and 2 facilitates a more physical interpretation of the observed long decay times. The lifetimes of the constant angle SPP modes are so short that these modes essentially decay within the pulse duration. On the other hand, the scattered light that has traveled some distance before coming back to the point of origin decays due to losses such as absorption along its propagation path (see Fig. 5). In principle the value of the diffusion coefficient for the SPP's in Ag and Au could be extracted through STM characterization of a roughness distribution function. This may also be done by systematically changing the size and concentration of scatterers, as was done in Refs. [3,4], although this would be a more difficult undertaking for surfaces.

The multiple scattering process has the effect of, over time, causing regions of net constructive and destructive interference of the wave amplitude; in the strong scattering regime this results in Anderson localization of the propagating mode [6,7]. In our previous STM measurement of SPP-induced photoemission from thin Ag films [21], we have observed photoemission with different orders in the incident light intensity (2nd order changing to 3rd order) and

Table 2
Calculated parameters and fitted temporal decay times for scattering model

	L (μm)	T (fs)	τ (fs)
Ag 50 nm	173	588	230
Ag 35 nm	59.3	201	70
Au 35 nm	46.0	156	56

L: the propagation length times 2, i.e., the 'amplitude' propagation length.
T: amplitude temporal decay time calculated from L by $T = L/v_g$ where v_g is the SPP's group velocity: $v_g = c(\epsilon_1' + \epsilon_2'^{1/2})/(\epsilon_1'\epsilon_2')$.

attributed this change of order to the SPP-assisted ionization response from different surface locations which have different work function. In case of SPP localization, it should be possible to observe different photoemission behaviors at different locations. For example, one may expect to to see enhanced photoemission from locations of constructive interference of SPP scattering amplitudes exist while no photoemission from locations of destructive interference.

5. Conclusion

Coherent multiple scattering of surface plasmon polaritons by surface features has been observed in room temperature deposited Ag and Au films (as compared to intentionally roughened films) through monitoring the interferometric interaction of the scattered light with a time delayed probe pulse. The signals can be fitted by a simple two dimensional photon diffusion model. The existence of coherent multiple scattering in these films supports the possibility of photon localization on these film surfaces. The temporal decay times of SPP's on rough surfaces are extracted from the experimental data. It is also worth noting that a diffusion model treatment is only a crude approximation to the microscopic phenomena. A more rigorous theoretical analysis would involve calculating the signals from the multiply scattered electromagnetic waves directly. However, this simple treatment provides a good framework to understand the experimental results.

Electromagnetic field localization in random scattering media is a subject attracting a great deal of current attention. The photon scanning tunneling microscopy work [5] has shown that a metal film surface may be a good candidate to study this phenomenon. Since coherent multiple scattering is the precursor to photon localization, we have presented further supportive evidence to photon localization on surfaces. Considering that local probe methods can be applied to surfaces, this may offer a unique system to study photon localization and make further comparisons to bulk systems. On the other hand, since many surface processes are enhanced by localized fields, the development of local probe methods [35] may now make possible the direct obsevation of the effect of localized fields on, for example, chemical reactivity of molecules adsorbed on surfaces or electrochemical reactions.

6. Note added

Since the review of this Letter, the femtosecond optical spectroscopy-SPM work of Ref. [21] has been extended to the tunneling gap regime. It has been possible to directly correlate femtosecond pulse photoinduced reactivity (i.e. the near-field analog of SPP-assisted ionization) to surface structural features with better than 10 nm precision and resolution. These studies were performed in the tunneling distance regime on Ag films with an insulated-tip STM, thereby facilitating simultaneous determination of the surface 'topography.' The results of these studies will be reported elsewhere.

Acknowledgements

The authors thank B. Romanow of the LRSM for providing the thin films used in this study. We acknowledge financial support from the University of Pennsylvania MRL (DMR-91-20668) and National Science Foundation SGER grant CHE-9311337 and grant CHE-9357424. NSF is an Arnold and Mabel Beckman Young Investigator and the recipient of a David and Lucille Packard Foundation Fellowship and is a Camille Dreyfus Teacher–Scholar.

References

[1] H. Raether, Springer Tracts in Modern Physics, Vol. 111, Surface Plasmons on Smooth and Rough Surfaces and on Gratings (Springer, Heidelberg, 1988).
[2] M. Specht, J.D. Pedarnig, W.M. Heckl and T.W. Hansch, Phys. Rev. Lett. 68 (1992) 476.
[3] C.K. Chen, A.R.B. de Castro and Y.R. Shen, Phys. Rev. Lett. 46 (1981) 145.
[4] C. Douketis, V.M. Shalaov, T.M. Haslett, Z. Wang and M. Moskovits, J. Electron Spectrosc. 64/65 (1993) 167.
[5] S.I. Bozhevolnyi, I.I. Smolyaninov and A.V. Zayats, Phys. Rev. B51 (1995) 17916; Opt. Comm. 117 (1995) 417.
[6] K. Arya, Z.B. Su and J.L. Birman, Phys. Rev. Lett. 54 (1985) 1559.
[7] P.-E. Wolf and G. Maret, Phys. Rev. Lett. 46 (1985) 2696.

[8] R. Vreeker, M.P. Van Albada, R. Sprik and A. Lagendijk, Phys. Lett. A132 (1988) 51, and references to earlier work from this group.
[9] G.H. Watson, Jr., P.A. Fleury and S.L. McCall, Phys. Rev. Lett. 58 (1987) 945.
[10] M. Rusek and A. Orlowski, Phys. Rev. E51, R2763 (1995).
[11] D.A. Boas, M.A. O'Leary, B. Chance and A.G. Yodh, Phys. Rev. E47 (1993) R2999.
[12] K.M. Yoo and R.R. Alfano, Opt. Lett. 15 (1990) 320.
[13] J.G. Fujimoto, S. De Silvestri, E. Ippen, C. Puliafito, R. Margolis and A. Oseroff, Science 254 (1991) 1178.
[14] A. Otto, Z. Phys. 216 (1968) 389.
[15] E. Kretschmann, Z. Phys. 241 (1971) 313.
[16] H.J. Simon and J.K. Guha, Opt. Comm. 18 (1976) 391.
[17] A.J. Braundmeier, Jr. and H.E. Tomaschke, Opt. Comm. 14 (1975) 99.
[18] V.M. Agranovich and D.L. Mills, Surface Polaritons (North Holland, Amsterdam, 1982).
[19] N. Kroo, W. Krieger, Z. Lenkefi, Z. Szentirmay, J.-P. Thost, and H. Walther, Surf. Sci. 331–333 (1995) 1305, and references to earlier work therein.
[20] R.H.M. Groeneveld, R. Sprik and A. Lagendijk, Phys. Rev. Lett. 64 (1990) 784.
[21] M.J. Feldstein, P.Vöhringer, W. Wang and N.F. Scherer, J. Phys. Chem. 100 (1996) 4739.
[22] K. Ema and M. Kuwata-Gonokami, Phys. Rev. Lett. 75 (1995) 224.
[23] P. Cong, Y.J. Yan, H. Deuel and J.D. Simon, J. Chem. Phys. 100 (1994) 7855.
[24] T.-S. Yang, P. Vöhringer, D. Arnett and N.F. Scherer, J. Chem. Phys. 103 (1995) 8346.
[25] T. Joo, Y. Jia and G.R. Fleming, J. Chem. Phys. 102 (1995) 4063.
[26] W.P. de Boeij, M.S. Pshenichnikov, K. Duppen and D.A. Wiersma, Chem. Phys. Lett. 224 (1994) 243.
[27] C. Bardeen and C.V. Shank, Chem. Phys. Lett. 226 (1994) 310.
[28] P. Leisching, J. Dekosky, C. Waschke, H. Roskos, K. Leo, H. Kurz and K. Kohler, in: Ultrafast Phenomena IX., ed. P. Barbara (Springer, Berlin, 1994) p. 337.
[29] E.J. Heilweil and R.M. Hochstrasser, J. Chem. Phys. 82 (1985) 4762.
[30] D.-S. Kim, J. Shah, J.E. Cuningham, T.C. Damen, S. Schmitt-Rink, and W. Schafer, Phys. Rev. Lett. 68 (1992) 2838.
[31] W.S. Fann, R. Storz and H.W.K. Tom, Phys. Rev. B46 (1992) 13592.
[32] R.V. Andaloro, H.J. Simon and R.T. Deck, Appl. Opt. 33 (1994) 6340.
[33] K.L. Kliewer and R. Fuchs, Adv. Chem. Phys. 27 (1974) 355.
[34] P.B. Johnson and R.W. Christy, Phys. Rev. B6 (1972) 4370.
[35] F. Zenhausern, Y. Martin and H.K. Wickramasinghe, Science 269 (1995) 1083.